Using Geometry to Detect Grasping Points on 3D Unknown Point Cloud

4 authors:

Brayan S. Zapata-Impata
Amazon
23 PUBLICATIONS   **246** CITATIONS

Carlos Mateo
University of Burgundy
26 PUBLICATIONS   **149** CITATIONS

Pablo Gil
University of Alicante
150 PUBLICATIONS   **1,420** CITATIONS

Jorge Pomares
University of Alicante
152 PUBLICATIONS   **1,635** CITATIONS

Some of the authors of this publication are also working on these related projects:

Project   Hacia una mayor integración de robots inteligentes en la sociedad: navegar, reco View project

Project   MISIONES CRÍTICAS DE EMERGENCIAS CON MEDIOS AÉREOS TRIPULADOS Y NO TRIPULADOS EN VUELO COOPERATIVO (ENJAMBRE) View project

Using Geometry to Detect Grasping Points on 3D Unknown Point Cloud

Brayan S. Zapata-Impata, Carlos M. Mateo, Pablo Gil and Jorge Pomares

Physics, System Engineering and Signal Theory, University of Alicante, 03690 Alicante, Spain

Computer Science Research Institute, University of Alicante, Alicante, Spain

Keywords: Grasping, 3D Point Clouds, Surface Detection, Handle Grasping, Unknown Object Manipulation.

Abstract: In this paper, we focus on the task of computing a pair of points for grasping unknown objects, given a single point cloud scene with a partial view of them. The main goal is to estimate the best pair of 3D-located points so that a gripper can perform a stable grasp over the objects in the scene with no prior knowledge of their shape. We propose a geometrical approach to find those contact points by placing them near a perpendicular cutting plane to the object's main axis and through its centroid. During the experimentation we have found that this solution is fast enough and gives sufficiently stable grasps for being used on a real service robot.

1 INTRODUCTION

The task of grasping objects using robots such as grippers have been widely studied in the state-of-art. Often, to accomplish autonomous robots and to specifically carry out the grasping task, the researchers use information acquired from visual sensors (Gil et al., 2016). In the past, the proposed approaches usually recognised the object in the scene from one or more views and later detected potential grasping points using a previously stored 3D model of that object. These points can be also computed considering the grasping problem as a classification task, where large datasets are required for training and testing.

In this paper, we use a single point cloud with a partial view of the objects present in the scene. Moreover, the objects are unknown, hence they have not been previously recognised and we have not a 3D model to compute candidate grasping points. Our main goal is to estimate the best pair of 3D-located points so that a gripper can perform a stable grasp over the object with no prior knowledge.

Recently, several authors have developed learning approaches to this problem by finding a gripper configuration using a grasping rectangle. (Jiang et al., 2011) introduced this idea representing a 2D oriented rectangle in the image with two of the edges corresponding to the gripper plates and the two other edges representing its width. Originally, the authors used RGBD images to find the optimal grasping rectangles by using a ranking linear function, learnt using a supervised machine learning algorithm.

Afterwards, this grasping rectangle has been learnt using deep learning techniques in recent years. Thereby, (Lenz et al., 2013) used RGBD images to train a deep neural network that generated a set of rectangles ranked by features obtained from the data contained inside the bounds of the grasping rectangle. In (Wang et al., 2016) the authors built a multimodal Convolutional Neural Network (CNN) instead.

Some authors have tested the grasping rectangle calculation using a different set of features apart from the RGBD channels. For instance, (Trottier et al., 2016) used RGBD images including more features like grey maps and depth normals. In (Redmon and Angelova, 2015), the authors' proposal consisted not on adding more channels to the images but on using only the Red, Green and the Depth one.

Although learning approaches have proved to be highly accurate, they require a significant amount of data and time to fine tune the learning architectures and the input features in order to be able to generalise.

Another frequently taken path to solve this problem consists on reconstructing a mesh from the seen object to compute the grasping points on complete CAD models or retrieve them from template grasps. In (Varley et al., 2015), the authors proposed a system that consisted on segmenting point clouds to find the objects in the scene, then they reconstructed meshes so the GraspIt! simulator (Miller and Allen, 2004) could find the best grasp configuration.

In (Vahrenkamp et al., 2016), authors proposed a database of grasps templates over segmented meshes. During online grasping calculation, the robot would

decompose the object's RGBD image in meshes of primitive forms to match them against the templates. Following this same idea, (Jain and Argall, 2016) proposed an algorithm to match real objects against geometric shape primitives, with fixed grasping strategies, using point clouds.

However, these solutions do not generalise well to unseen objects since they are restricted to those forms previously recorded and they need additional views in order to reconstruct correctly the objects.

As for using point clouds and not only RGBD images, (Richtsfeld and Vincze, 2008) proposed a method for computing a pair of grasping points over point clouds. Firstly, they searched for the top planar surface of the object and then picked the closest point in the rim to the object's centre of mass. The second grasping point was on the opposite rim. Similar to this geometric approach, (ten Pas and Platt, 2015) computed grasping candidates analytically locating antipodal grasps. This work was later followed by another approach where the authors localised hand-like areas in the object's cloud (ten Pas and Platt, 2016).

On this paper, we present a novel algorithm for robotic grasping with grippers capable of detecting grasping points on unknown objects using a single point cloud view. This method automatically segments the point cloud to detect the objects present in the scene. Then, for each of them, it calculates a set of contacting points that fulfil certain geometric conditions and ranks their feasibility to find the most stable grasp given the view conditions.

The rest of the paper is ordered as follows: section 2 describes the robotic hand constraints and the objects geometry as well. Section 3 details the method used for segmenting the input cloud, finding the candidate grasping points areas and ranking them for selecting the best grasping pair of points. Section 4 shows the results obtained using a dataset of everyday objects and section 5 presents our conclusions.

2 GEOMETRIC AND KINEMATICS CONSTRAINTS

2.1 Hand Kinematic

For this work, we take into account only the physical limitations of a robotic hand for testing the contact points generated. The hand used is the Barrett hand, shown in figure 1. This hand is an underactuated grasper typically used in industrial scenarios with three fingers, two of them that spread, counting with 4 degrees of freedom.
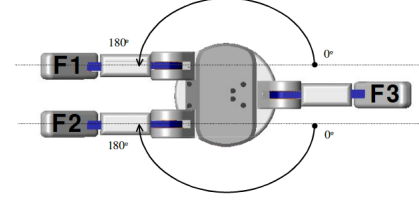

Figure 1: Barrett robotic hand. Reproduced from (Townsend, 2000).

In this work, we will use only two fingers, F1 and F3, as a gripper. The maximum working aperture $gripper\_max\_amp$ of this hand is equal to 335mm and their tip width $gripper\_tip\_width$ is equal to 25mm. These attributes will influence the contact points calculation.

2.2 Object Geometry

We use for this work opaque, rigid objects which have at least one dimension smaller than the maximum working aperture of the robotic gripper. These objects are restricted to be opaque due to the limitations of the depth camera used with which RGBD images are acquired using projected coded IR patterns. Transparent objects or dark ones would not be detected properly due to the wavelength of the emitted light that can be reflected or refracted by some materials.

As for their stiffness, we are not dealing with deformable bodies nor objects with holes passing through them (all objects are compacts). This assumption is required in order to avoid deformations or noise that would affect the calculation.

3 GRASPING POINT SELECTION

In order to select the best grasping points for the gripper, we first need to segment the scene where the objects are presented. Then, a candidate area in the objects surface is found for each of the plates and combinations of points from these areas are ranked using a custom function so the best configuration can guarantee the most stable grasp under the view conditions.

3.1 Scene Segmentation and Object Detection

Given a recorded point cloud C, we first need to detect objects in the scene. In order to do so, we begin by filtering out points $p \in C$ whose z-component fulfil $p_z > 1m$ so we are left only with points closer to the camera. Then, the ground plane Π_g, where objects are laying, is detected with RANSAC (Fischler and Bolles, 1981). Once the points $p \in \Pi_g$

155

Figure 2: Scene segmentation. (left) original registered point cloud, (right) detected objects after plane segmentation and clusters detection.

are extracted from C, an Euclidean Cluster Extraction (Rusu, 2010)(Rusu and Cousins, 2011) is passed to detect each of the objects point clouds C_k. The results of this process are displayed in figure 2.

3.2 Grasping Areas

Afterwards, an object to be grasped is selected. Its point cloud C_k is preprocessed to filter outliers from its surface. Next, the centroid of C_k is computed. In addition, the main axis $\vec{v}$ of the cloud is obtained in order to approximate the object's largest axis. Having done so, a cutting plane Π perpendicular to such direction $\vec{v}$ through the object's centroid is calculated. In the intersection of the plane Π and the cloud C_k, we subtract a set of points $\gamma \subset C_k$ that are within 1cm to the plane Π, being this distance the best one found empirically.

If the object's axis $\vec{v}$ is parallel to the ground plane Π_g, the points located in the two opposite areas along the Z axis of the camera are the candidate grasping points. Otherwise, the candidates are in the opposite sides of the X axis from the camera viewpoint. The Y axis is avoided since it includes the object's points in contact to the ground plane Π_g.

In order to find these candidate grasping points, the points $p_{min} \in \gamma$ and $p_{max} \in \gamma$ with the minimum and maximum component value (X or Z depending on the case) are selected. This way, two candidate points clouds C_{min} and C_{max} are extracted using two spheres S_{min} and S_{max} centred in p_{min} and p_{max} respectively. Their radius are initially equal to $r = 2 * gripper\_tip\_width$, being $gripper\_tip\_width$ the gripper's plate width in millimetres. However, in case the object's width $w_{obj} = L^2norm(p_{min}, p_{max})$ fits the condition $w_{obj} \leq 2 * r$, then $r = \frac{w_{obj}*0.9}{2}$ to adapt the grasp area to the object's size.

$$L^2norm(p,q) = \sqrt{\sum_{i=1}^{n}(p_i - q_i)^2} \quad (1)$$

Based on this, the candidate point clouds C_{min} and C_{max} include those points belonging to the object's cloud C_k which are within the volume of the
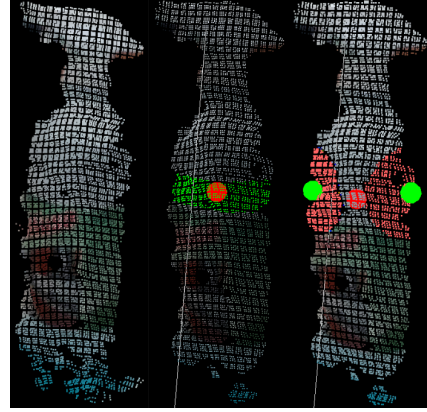

Figure 3: Grasping areas detection. (left) original object's point cloud C_k, (middle) filtered cloud, centroid detected as a red sphere, object's axis $\vec{v}$ as a white line and cutting plane Π represented in green, (right) initial points p_{min} and p_{max} in green as well as candidate points clouds C_{min} and C_{max} coloured in red.

sphere S_{min} and S_{max}. That is, $C_{min} = S_{min} \cap C_k$ and $C_{max} = S_{max} \cap C_k$. In figure 3, we show the process of detecting the grasping areas.

3.3 Grasping Points Ranking

As for ranking a grasp configuration $\Theta = \{p_1 \in C_{min}, p_2 \in C_{max}\}$, we propose a function that evaluates their stability depending on the following factors:

1. **Distance to the Grasp Plane Π:** this plane is cutting the object through its centroid so the closer the grasping points p_1 and p_2 are to the plane Π, the closer they are to a reference to the object's centre of mass. This could be translated to an equilibrated grasp. This distance is obtained as:

$$distance(\Pi, p) = abs(\vec{n} \cdot p + offset) \quad (2)$$

where $\vec{n}$ is the unitary normal vector of the plane Π, p is one of the grasping points p_1 or p_2 and $offset$ is the distance of the plane Π to the origin.

2. **Point's Curvature:** the curvature measures the variations on the object's surface. A grasp is likely to be more stable if it is executed over a planar area instead of highly curved points. In particular, the point's curvature measures the variation between this one and its neighbours on the same surface. Both, the size (radius of sphere) and the number of points (dense of sphere) influence the estimation of the curvature values. To estimate the curvature, we apply the method presented in (Pauly et al., 2002). Thereby, we first compute the covariance matrix of points within the sphere and

obtain the eigenvalues and eigenvectors from Singular Value Decomposition (SVD). The covariance matrix is previously obtained from a Principle Component Analysis (PCA). Later, the eigenvalues sum supplies surface variation information between each point of the sphere and its centroid and, the smallest eigenvalue gives us the variation along the normal vector to the surface. Accordingly, the curvature can be computed as:

$$\lambda_p = \frac{\lambda_0}{\lambda_0 + \lambda_1 + \lambda_2} \quad (3)$$

where λ_p is the curvature on the point p, λ_i is each eigenvalue of the covariance matrix being $i = 0$ the smallest and $i = 2$ the biggest eigenvalue, respectively.

3. **Antipodal Configuration:** in an antipodal grasp the gripper is able to apply opposite and collinear forces at two points. In this case, a pair of contact points with friction is antipodal if they lay along a line parallel to the direction of finger motion. To guarantee this, the angle α between the ith-contact point's normal $\vec{n}_i$ and the line $\vec{w}$ connecting p_1 and p_2 should be close to zero.

4. **Perpendicular Grasp:** since the grasping areas are spherical, there are chances for a candidate grasp to not be parallel to the cutting plane Π. In order to avoid trying to execute slippery grasps, we penalise those configurations which are not parallel to the cutting plane Π. That is, the line $\vec{w}$ which connects the grasping points p_1 and p_2 should have an angle β with the cutting plane's normal $\vec{n}$ close to 90 degrees.

Assuming these conditions, the following is the proposed ranking function for a grasp Θ:

$$
\begin{aligned}
rank(p_1, p_2) =& w1 * r1(p_1, p_2) + w2 * r2(p_1, p_2) \\
r1(p_1, p_2) =& 1.0 - dis(\Pi, p_1)^2 + 1.0 - dis(\Pi, p_2)^2 + \\
& 1.0 - cos(\beta) \\
r2(p_1, p_2) =& 1.0 - \lambda_{p_1} + 1.0 - \lambda_{p_2} + \\
& cos(\alpha_{p_1}) * cos(\alpha_{p_2})
\end{aligned}
$$

$$(4)$$

where $dis(\Pi, p_i)$ is the distance of the grasping point p_i to the grasp plane Π as measured in equation (2), and λ_{p_i} is the curvature of the grasping point p_i as measured in equation (3), and α_{p_i} is the angle between the ith-grasping point's normal $\vec{n}_i$ and the connecting line $\vec{w}$, and β is the angle between the cutting plane's normal $\vec{n}$ and the connecting line $\vec{w}$.

We split our function *rank* in two sub-functions *r1* and *r2* because they evaluate distinct attributes of

the grasp configuration Θ. As for *r1*, it evaluates the geometrical position of the grasping points over the object's surface. The curvature characteristics of their area are evaluated by *r2*. These two natures are then weighted using *w1* and *w2* to balance their influence in the ranking function. In this work, $w1 = w2$ so both factors have the same importance.

The values included in this ranking function are all in the range $[0, 1]$ so ranking values vary in the range $[0, 6]$, being 6 the score given to best grasp configurations while unstable ones are closer to 0. In addition, point cloud normal vectors and curvatures are calculated previously using a a radius $r = 3cm$.

Furthermore, these candidate areas C_{min} and C_{max} are voxelised so that the calculus can be made faster. It is not necessary using every single candidate point because if a point has for example a high curvature value, its neighbours are likely to be under very similar conditions. Thus, voxels are used as a representation of a tiny surface inside the candidate grasping area. These voxels are computed using a radius dependant of the gripper's tip width in a factor of $voxel\_radius = gripper\_tip\_width * 0.5$.

4 EXPERIMENTS

For this experimentation, we have acquired point clouds using a RealSense SR300 depth camera. The dataset of objects is composed of the following household objects: milk brick, toothpaste box, cookies box, spray bottle, bowl, mug, plastic glass, book, can, tennis ball, deodorant roll-on, pillbox and telephone. These objects and the scene view from the camera are presented in 4. Objects lay in a range from 40cm to 100cm from the camera base.

Our algorithm was implemented in C++ using the library PCL 1.7 and tested on an Intel i7-4770 @ 3.4 GHz x 8 cores with 8 GiB of system memory. For

Figure 4: Experimentation set comprised of 13 objects.

Table 1: Average grasp feasibility as a percentage and rank value for each object presented in isolation.

Object	Dimensions (mm)	# Views	f_{robot}	f_{env}	$r1$	$r2$	$rank$
Toothpaste	46x190x38	6	1.00	1.00	2.38	1.04	3.42
Cookies	305x210x48	8	1.00	0.75	2.60	1.36	3.96
Milk	97x195x58	6	1.00	1.00	2.38	1.77	4.15
Book	123x202x25	6	1.00	0.83	2.72	1.33	4.05
Pillbox	58x77x37	6	1.00	1.00	2.51	1.11	3.62
Can	65x115x65	4	1.00	0.75	2.20	1.86	4.07
Roll-on	46x102x46	4	1.00	0.75	2.28	0.92	3.20
Spray	80x290x80	4	1.00	0.75	2.31	1.63	3.94
Mug	82x96x82	5	1.00	1.00	2.66	1.91	4.57
Glass	79x107x79	5	1.00	1.00	2.35	1.40	3.75
Bowl	172x78x172	4	1.00	0.75	2.76	2.08	4.84
Ball	63x63x63	2	1.00	1.00	2.80	1.57	4.38
Telephone	49x157x23	5	0.80	0.80	2.16	1.40	3.56

real time testing, it was implemented in ROS as a subscriber node that read the camera data directly.

In the experiments, we will evaluate f_{robot} as the grasps feasibility constrained only to the hand limitations by calculating the distance between the grasping points. If it requires to open the gripper a smaller width than its maximum operating amplitude *gripper_max_amp* but they are not closer than a minimum distance, it is scored as a feasible grasp. Otherwise, it is not physically possible to grasp it. For this purpose, we have used *gripper_tip_width* as the minimum and *gripper_max_amp* as the maximum opening width, being these the physical limitations of the Barrett hand described in section 2.1.

Furthermore, the f_{env} metric will evaluate the feasibility of the grasp taking into account the environmental constraints. For example, if a grasp requires pushing the robotic hand under the object or both contact points lay in the same surface the robot will collide so it will be scored as infeasible.

4.1 Objects Presented in Isolation

For this experiment, the dataset objects were placed alone on the table at a sufficient distance to be properly detected by the camera. In case of smaller objects like the pillbox or the ball this requires them to be closer than bigger ones like the cookies box. Various poses were taken and the proposed grasping algorithm was run. In the table 1 we present the obtained results.

Our dataset of objects is comprised of household objects that can be categorised in some geometrical types like boxes, cylinders and spheres. Box-like objects were laid down in different positions so each time the camera would acquired a new view of it. Cylinders were laid down parallel to the Z axis,

as well as X axis and in diagonal to both of them. Spheres are equally seen from every point of view so they were moved along the Z axis to bring them closer and further to the camera.

It can be observed that $r1$ usually contributes with at least 2 out of 3 points to the ranking function. This means that our ranking function is able to find good contact points near the cutting plane that are parallel to it. In our hypothesis, grasps parallel and close to the cutting plane Π will be more stable since they will be closer to the point cloud centroid, that can be used as a representation of the object's centre of mass. Grasping closer to this point leads to more equilibrated grasps if the object's is proportionally dense through its whole body, something that can be said for most of the household objects a service robot would manipulate.

Regarding $r2$, we have tested that box-like objects tend to have lower scores on this function than cylinders or spheres. In this function, we are ranking the curvature of the contact point area and if they configure an antipodal grasp as well. Planar objects will have lower curvature values so it is logical to think that these objects should have greater $r2$ values. However, due to only using one viewpoint of the object, it is difficult to find more than two faces of boxes in the same point cloud, making the configuration of an antipodal grasps complicated. In order to configure one, contact points should lay in two planes of the box with normal vectors in the same direction but counter-wise. Since this is not the case, our box grasps are penalized by not configuring an antipodal grasp.

We have observed that the closer the objects are to the camera, the more dense their point clouds are and more information is available about its surface. That results in higher ranked configurations due to having more points to work with. That is, views that propor-
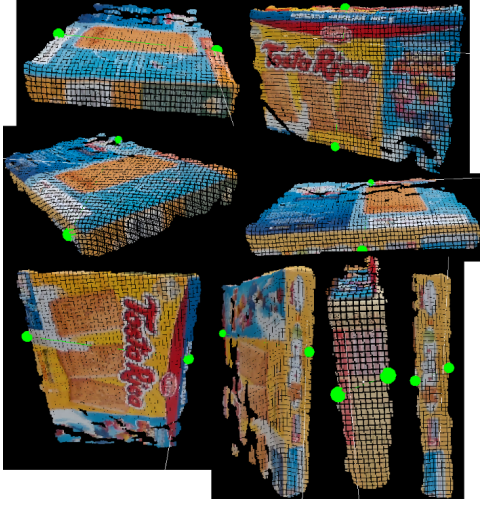
Figure 5: Samples of grasps calculated by the proposed algorithm over the cookies box in different poses.

Table 2: Average objects presented in reality/detected, the feasibility of their grasps and the rank for each object.

Scene	# R/D	f_{robot}	f_{env}	rank
Cylinders	6/5	1.00	0.60	3.55
Laying	7/7	1.00	0.71	3.97
Box-sphere	8/8	1.00	1.00	4.00
Cyl-sphere	8/7	0.85	0.85	4.16
Mix10-a	10/9	0.88	0.88	3.92
Mix10-b	10/10	1.00	0.90	4.01
Mix12-a	12/11	1.00	0.90	4.28
Mix12-b	12/12	1.00	0.91	3.73
Dataset-a	13/13	1.00	1.00	3.53
Dataset-b	13/14	1.00	0.78	3.68

tion more information about the object's shape facilitate finding better contact points.

Although the algorithm is designed to avoid recommending infeasible grasps like those that require contacting the object through its lower surface, sometimes the recording conditions leads to grasps that cannot be performed. As is shown in the table 1, f_{robot} is usually equal to 100% meaning that every proposed grasp is physically possible for our robotic hand. However, during this experimentation, we found a proposed grasp for the telephone that required positioning the grippers so close that they would collide. This fact was due to displaying a lateral view of the telephone that was very thin so any proposed grasp using such view required placing the grippers too close.

As for f_{env}, it has been proved that sometimes, the algorithm proposes grasps that are placed beneath the objects, like the one displayed in the top right corner in figure 5. We have checked that this fact usually happens because the detected object's main axis is parallel to the table and there is enough noise to find smaller Z values in lower parts than in the top of the object so the initial point p_{min} is placed wrong. This is a case that our proposal treats incorrectly due to the point cloud conditions.

4.2 Objects Presented in Clutter

In most of the real situations, the robot would face, objects will not be isolated and they may be partially occluded or surrounded by others. In these experiments, we have distributed the dataset of all objects on the work-table surface. In the table 2, we present the results obtained by evaluating how many objects were presented in real, how many were detected and

how many had a feasible grasp calculated as well as their mean rank.

We do not present these experiments in dense clutter with objects contacting each other since that would make the task of segmenting the objects using the point cloud more difficult. Since we are not evaluating an object detection algorithm nor we are proposing one, the objects presented in these experiments are sufficiently separated to allow us test our contact points calculation while still being in clutter.

Generally, all objects in the scene can be seen and therefore detected. However, sometimes some objects are missed since they are too occluded or small that do not seem an object for the algorithm. Regarding the objects detected, now that they are partially occluded the rate f_{env} decreases. Most of the erroneous proposed grasps are due to being over objects in the back so they are not properly seen or because the segmenting algorithm confuses two objects and mixes them in the same object. These cases are displayed in the figure 6, where in the Mix12-a scene the toothpaste and milk boxes are mixed in one single object. The same happens in the Mix10-a scene with the mug and the milk box.

Another issue for discussing is that when an object is in front of another one, the object in the back can be seen as two different point clouds. This fact is the case of the milk box in the scene Dataset-b in the figure 6. If those two boxes were separated objects, it could be said that our algorithm is proposing two feasible grasps. However, we know those grasps cannot be executed. In a common clear-the-table task, we would pick the toothpaste box and then recompute grasps for the visible objects, solving this situation by doing so.

4.3 Real Time Testing

Apart from evaluating the contact points feasibility of our proposed algorithm, we have tested its speed. For this experiment, we have saved in rosbags 5 seconds

Figure 6: Samples of grasps proposed over clutter scenes. Top: (left) Mix12-a, (right) Mix10-a. Bottom: (left) Dataset-b, (right) Cyl-sphere.

of point clouds from our camera. Several objects configuration were tested including the case of one single object but with different sizes and a growing distribution where the whole dataset of objects was introduced one by one in each scene. Results are presented in table 3.

As was expected, the average time needed to compute the contact points for a single object depends on its size. More specifically, it depends on the amount of points processed. Bigger objects tend to have bigger point clouds so they are slower to process.

If just one single object is presented in the scene the algorithm reaches a frames per second (FPS) rate greater than 1. However, checking the dataset scenes it can be observed that as we introduce more objects

Table 3: Average time calculating contact points for each object in the scene and frames per second (FPS).

Scene	# Objects	Time/Object (ms)	FPS
Cookies	1	530.00	1.30
Milk	1	45.61	11.45
Ball	1	26.94	17.13
Dataset	1	213.73	3.16
Dataset	2	126.04	2.84
Dataset	3	95.45	2.51
Dataset	4	80.08	2.10
Dataset	5	63.24	1.89
Dataset	6	84.00	1.19
Dataset	7	95.38	1.19
Dataset	8	96.24	1.10
Dataset	9	79.13	1.05
Dataset	10	84.03	0.92
Dataset	11	88.50	0.85
Dataset	12	78.60	0.81
Dataset	13	88.25	0.73

the proposed algorithm for detecting the objects and then calculating their grasping points takes more time, reducing the FPS rate. Nevertheless, the time required to calculate a single pair of contact points is lowered because we keep introducing more objects and then bigger ones become occluded so their point clouds are also reduced. This issue is also an effect of beginning this test with greater objects at the back like the cookies box of the spray and then keep introducing smaller one in front of them so they can be easily detected.

Any single tested object took more than 1 second to be detected and processed to give a grasp configuration. Therefore, it is fast enough to be used in a real implementation as the grasping points calculation system of a service robot.

5 CONCLUSIONS

In this paper, we propose a new algorithm for grasping novel objects with robotic grippers using 3D point clouds and no prior knowledge. The main idea is to geometrically find regions that fulfil a set of basic conditions. These regions are found by calculating the object's main axis and its centroid. Then, a cutting plane perpendicular to such axis and that holds the object's centroid is computed. This cutting plane defines in the extremes of the object two candidate areas for placing the gripper plates. Configurations of points combined from both areas are then ranked in order to find the most stable and feasible grasp, taking into account their geometric positions in respect to the cutting plane and their curvature characteristics.

Due to depending on the previous segmentation of the scene and the calculation of the object's main axis, it is badly influenced by noise and poor point of views of the objects to be grasped. Despite this fact, it is still able to find always a pair of grasping points in less than one second and stays as a useful basic contact points calculation system.

In future work, we would like to extend it to make full use of robotic hands with more than two fingers as well as study a way to dynamically change the influence of $r1$ and $r2$ in the *rank* function by modifying theirs weights $w1$ and $w2$. In addition, we want to test this ranking function as a measure of the point of view quality in terms of the best grasping points that can be computed from it.

ACKNOWLEDGEMENTS

REFERENCES

Fischler, M. a. and Bolles, R. C. (1981). Random Sample Consensus: A Paradigm for Model Fitting with Applicatlons to Image Analysis and Automated Cartography. *Communications of the ACM*, 24(6):381 – 395.

Gil, P., Mezouar, Y., Vincze, M., and Corrales, J. A. (2016). Editorial: Robotic Perception of the Sight and Touch to Interact with Environments. *Journal of sensors*, 2016(Article ID 1751205):1–2.

Jain, S. and Argall, B. (2016). Grasp detection for assistive robotic manipulation. *Proceedings - IEEE International Conference on Robotics and Automation*, 2016-June:2015–2021.

Jiang, Y., Moseson, S., and Saxena, A. (2011). Efficient grasping from RGBD images: Learning using a new rectangle representation. *Proceedings - IEEE International Conference on Robotics and Automation*, pages 3304–3311.

Lenz, I., Lee, H., and Saxena, A. (2013). Deep Learning for Detecting Robotic Grasps. pages 1–4.

Miller, A. T. and Allen, P. K. (2004). GraspIt! *IEEE Robotics & Automation Magazine*, 11(4):110–122.

Pauly, M., Gross, M., and Kobbelt, L. (2002). Efficient simplification of point-sampled surfaces. *13th IEEE Visualization conference.*, (Section 4):163–170.

Redmon, J. and Angelova, A. (2015). Real-time grasp detection using convolutional neural networks. *2015 IEEE International Conference on Robotics and Automation (ICRA)*, pages 1316–1322.

Richtsfeld, M. and Vincze, M. (2008). Grasping of Unknown Objects from a Table Top. *Workshop on Vision in Action: Efficient strategies for cognitive agents in complex environments.*

Rusu, R. B. (2010). Semantic 3D Object Maps for Everyday Manipulation in Human Living Environments. *KI - Kunstliche Intelligenz*, 24:345–348.

Rusu, R. B. and Cousins, S. (2011). 3D is here: Point Cloud Library (PCL). *Proceedings - IEEE International Conference on Robotics and Automation*, (April).

ten Pas, A. and Platt, R. (2015). Using Geometry to Detect Grasps Poses in 3D Point Clouds. *Int'l Symp. on Robotics Research.*

ten Pas, A. and Platt, R. (2016). Localizing handle-like grasp affordances in 3D point clouds. *Springer Tracts in Advanced Robotics*, 109:623–638.

Townsend, W. (2000). The BarrettHand grasper- programmably flexible part handling and assembly. *The International Journal of Industrial Robot*, 27(3):181–188.

Trottier, L., Giguère, P., and Chaib-draa, B. (2016). Dictionary Learning for Robotic Grasp Recognition and Detection. *arXiv preprint*, pages 1–19.

Vahrenkamp, N., Westkamp, L., Yamanobe, N., Aksoy, E. E., and Asfour, T. (2016). Part-based Grasp Planning for Familiar Objects. *2016 IEEE-RAS International Conference on Humanoid Robots (Humanoids 2016)*.

Varley, J., Weisz, J., Weiss, J., and Allen, P. (2015). Generating multi-fingered robotic grasps via deep learning. *IEEE International Conference on Intelligent Robots and Systems*, 2015-Decem:4415–4420.

Wang, Z., Li, Z., Wang, B., and Liu, H. (2016). Robot grasp detection using multimodal deep convolutional neural networks. *Advances in Mechanical Engineering*, 8(9):1–12.